Cellular metals

Anthony G Evans*, John W Hutchinson* and Michael F Ashby†

The property profile exhibited by cellular metals identifies several applications, especially in technologies requiring multifunctionality. Their specific property attributes suggest implementation as: ultralight panels/shells, energy absorbing structures and heat dissipation media as well as for vibration control. Connections between the properties that govern these performance benefits and the cellular architecture, cell morphology and density have been made. Such structural relations facilitate choices of optimum cell characteristics for defined multifunctional applications.

Addresses
*Division of Engineering and Applied Sciences, Harvard University, Cambridge, MA 02138, USA
†Engineering Department, Cambridge University, Cambridge CB2 1PZ, UK

Abbreviations

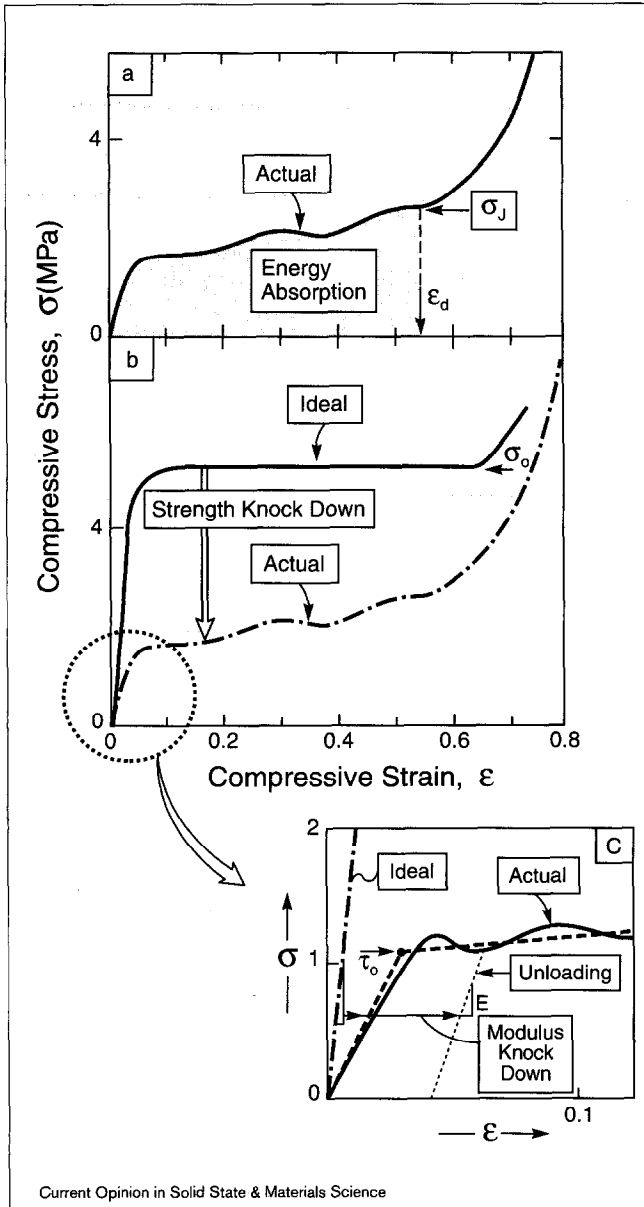|	
A_i	bending coefficients
b	thickness of foam
B	panel width
Bi	Biot number
c	core thickness
d	diameter of open cell ligaments
E	Young's modulus of cellular material
E_f	E for face sheets
E_s	E for cell walls
h	local heat transfer coefficient
H	global heat transfer coefficient
k	thermal conductivity of cell wall material
k_{eff}	effective thermal conductivity for cellular medium
l	heat transfer length
L	length of loaded structure
P	load
R	radius of shell
S	stiffness index
T	temperature of solid
T_f	fluid temperature
U	energy absorbed per unit volume (kJ/m^3)
U_p	energy absorbed per unit mass (J/g)
v	fluid velocity
W	minimum weight of structure
α	mechanical property coefficient
α_1	α for closed cell material stiffness (1)
α_2	α for open cell material stiffness (2)
α_3	α for closed cell material yield strength (3)
α_4	α for open cell material yield strength (4)
δ	displacement upon lateral loading of panel
ε	strain
ε_d	densification strain
κ	kinetic energy
λ_i	proportionality constants for effective thermal properties
Π	load index
ρ	relative density of cellular material
σ	stress
σ_o	yield strength of cellular material
σ_l	plateau compression strength
σ_s	yield strength of cell wall material
σ_Y	yield strength of face sheets
Ω	density of cell wall material
Ψ	weight index

Introduction

Metallic foams ('metfoams' or cellular metals) are a class of material unfamiliar to mechanical engineers [1•,2•]. They are made possible by a range of novel processing techniques, many of which are still under development. At present, metfoams are inadequately characterized. Moreover, process understanding and control are incomplete, resulting in variable properties. Yet, even the present generation of metfoams suggests alluring potential [3,4•,5,6,7•,8,9], as process control and characterization rapidly improve. Metfoams have potential in structures that are both light and stiff, for the efficient absorption of energy, for thermal management and perhaps for acoustic control and other, more specialized, applications. They hold, too, the promise for market penetration in applications where several of these functions can be combined. Implementation relies not just on properties, but on additional attributes: such as low manufacturing cost, environmental durability and fire retardancy.

Such materials have been available for decades [10,11], but new opportunities are now emerging for two reasons. Firstly, novel manufacturing approaches have beneficially affected performance and cost [P1–P3,12,13,14•]. Secondly, higher levels of basic understanding about mechanical, thermal and acoustic properties have been developed [2•,15•,16–19] in conjunction with associated design strategies [2•,3,4•]. These provide an integrated pathway between manufacturing and design. The literature is still sparse. Anyone interested in the field must read the book on 'Cellular Solids' by Gibson and Ashby [1•]. This book provides a comprehensive assessment of many types of cellular materials, with evident consequences for metal foams. But, cellular metals also have several unique characteristics and accordingly, this book should be supplemented by other readings. The patent literature is pertinent [P1–P3], as well as two progress reports [20,21] and the 'Ultralight Metals Web' page [22]. There is also a good review on manufacturing methods [10] (though now outdated). A 'Cellular Metal Design Manual' [2•], with associated software and data bases [5], will be available soon. This manual will embrace a full spectrum of properties, applications, design rules and case studies.

The stress/strain response exhibited by low density cellular metals establishes 'two aspects of their engineering utility', as is summarized in Figure 1. Firstly, the high stiffness and yield strength achievable at low density, relative to competing materials/systems, creates an opportunity for ultralight structures, with integrally-bonded dense face sheets [9]. Secondly, large compressive strains

Figure 1

Current Opinion in Solid State & Materials Science

(a) Actual stress and (b) ideal (σ)/strain (ε) curves for a closed cell Al-alloy indicating the knockdown factors. Also shown in (c) the inset is the definition used for the yield strength.

achievable at nominally constant stress (before the material compacts) imparts a high energy absorption capacity at force levels of practicable relevance for crash and blast amelioration systems [2•,9].

Open-cell metals constitute a third opportunity. These materials have thermal attributes that enable applications as heat dissipation media and as heat recuperators [6,7•]. The attributes include the high thermal conductivity of the material comprising the borders, in combination with a high internal surface area and propitious fluid transport dynamics, which enable high heat transfer rates that can be

used effectively for either the cooling of high power density devices or efficient heat exchange.

Cellular metals incorporated within a structure to form sandwich skins can result in systems that achieve mechanical performance and affordability goals at lower weights than competing concepts [4•] such as rib or waffle stiffened designs. Structural analysis of prototypical systems identifies those sandwich constructions which have explicit weight advantages. Such advantages are found in structures controlled by bending or compression, but not in those dominated by tension. For instance, in aircraft design about half of the structure is limited by its bending or compressive performance.

The benchmarks for comparison with sandwich skin construction comprise: firstly, stringer-stiffened panels or shells; secondly, honeycomb panels; and thirdly, hollow tubes [3,4•; MY He, JW Hutchinson, unpublished data]. Through decades of development, all three have been optimized and provide performance targets that are difficult to supersede. The principal literature in this area dates back to the postwar period (1940s and 1950s) [3,23–25]. "Benefits of sandwich construction with cellular metal cores derive from an acceptable structural performance combined with lower costs or greater durability than competing concepts". For example, honeycomb panels comprising polymer composite face sheets with an Al-honeycomb core are particularly weight efficient: they can never be superseded by cellular metal construction strictly on a performance basis. Such honeycombs have durability problems associated largely with water intrusion and they are relatively expensive [26]. They are also highly anisotropic and costly to configure as cores for curved structures.

Structures that absorb energy have two dominant properties [1•,2•]: the energy per unit mass, U_ρ (in J/g), and the stress at which this energy is absorbed, σ_J (Figure 1). 'High energy absorption is required at a predictable and uniform σ_J'. The latter metric ensures that the force transmitted to the underlying structure as the energy is being absorbed remains below a critical level, that upon impact/blast might otherwise cause structural damage. The former governs the foam thickness needed to absorb the kinetic energy. The first published work on cellular metals deals with this behavior [11].

Making metal foams

Generic manufacturing processes were reviewed in 1984 [10]. Metal foams are now made by one of seven basic processes:

1. Bubbling gas through molten Al–SiC or Al–Al$_2$O$_3$ [P3]. Foams of this type are made by three manufacturers: ALCAN, CYMAT and HYDRO. The range of materials is limited and the cell size tends to be large; but the process is intrinsically cheap.

2. Consolidation of a metal powder (typically an aluminum alloy) with a particulate foaming agent (typically TiH_2) followed by heating into the mushy state upon which the foaming agent releases hydrogen, expanding the material [P2]. The expansion can be done in a closed mold giving structures of complex shape with a dense outer skin. Such foams are manufactured by two producers: MEPURA and FRAUNHOFER.

3. By stirring a foaming agent (TiH_2 again) into a molten alloy (again, aluminum alloys are the most common) and controlling the pressure while cooling [P1]. The foaming agent is dispersed by stirring, releases gas and expands the metal. The foam made by Shinko Wise with the trade-name, ALPORAS, notable for its relative uniformity, is made in this way.

4. Pressure infiltration of a ceramic mold made from a polymer foam precursor, which is burned out before the metal is injected [10]. The process has considerable flexibility and enables the fabrication of foams from many different metals. The resulting structure is regular and reproducible, has open-cells, and a typical relative density of ~0.1. The foams available from Energy Research and Generation (ERG, Oakland, CA) are made by refinements of this process and the 'Lattice Block' materials made by JAMPcorp (Boston, MA) [27] use this process.

5. Vapor phase or electro-deposition onto a polymer foam precursor, which is subsequently burned out. The result is an open-cell metal foam with hollow cell edges (B Krizt, MF Ashby, unpublished data). The process developed by the International Nickel Corporation (INCO) works in this way.

6. Expansion of an inert gas trapped in pores at high pressure when a powder compact is hot isotatically pressed (HIPed; [12,13]). In the Boeing process, for example, Ti-alloy powder is HIPed in a sealed can with an initial pressure of ~3 MPa argon in the pores. The HIPed product is rolled into a sheet with the can material forming dense faces. The sheet is reheated to expand the trapped gas in the original powder layer giving a sandwich structure with a core porosity of ~30%.

7. Sintering of hollow spheres made by either a modified atomization process or by the sintering of a metal oxide (hydride), followed by reduction to the metal. Hollow Cu, stainless steel and Ti-6%Al-4%V spheres can be produced by this method. The MURILITE material is also made in this way (D Sypeck, HGN Wadley, personal communication), as is the Georgia Tech. material [14*].

Scaling relations
Generalities
Mechanical property scaling relations have been established by Gibson and Ashby [1*]. Results pertinent to metals are emphasized here [2*]. Distinctions are made between open-

and closed-cell materials which have inherently different characteristics. Specific responses are fundamentally related to bending and stretching deformations [1*]. Cellular elements that allow bending are subject to high local stresses that cause the system to be compliant and have a low yield strength. Conversely, when the cell walls stretch without bending, the system is stiff and has high strength.

Various high performance cell morphologies that minimize bending deformations have been conceptualized [7*,23,27]. Three examples include: periodic tetrakaideca-hedra [15*], close-packed-bonded spheres [19], and truss structures [27]. Most commercially available materials have inferior mechanical properties.

In ideal cellular materials, plastic yielding and collapse occur simultaneously [1*] resulting in a distinct yield strength coincident with a plateau flow stress, designated σ_0 (Figure 1). In commercial materials, yielding and collapse are not coincident [18]. Local yielding initiates at cell nodes almost immediately upon loading, followed by rapid strain hardening, resulting in narrow deformation bands that extend across the test configuration. Accordingly, the elastic domain is confined to very small strains (<0.1%). Thereafter, a peak develops with subsequent oscillation of the stress about a nominal plateau. The peak is governed by plastic collapse within one of these deformation bands. For expediency, the peak stress is defined as the yield strength, σ_0 (see Figure 1). Unloading measurements are preferred for determining the elastic properties because of anelastic effects on loading.

Stiffness
Closed cell structures establish upper limits on stiffness. At low relative densities, the Young's modulus, E, of such structures scales theoretically [1*,15*,16,19,28] as :
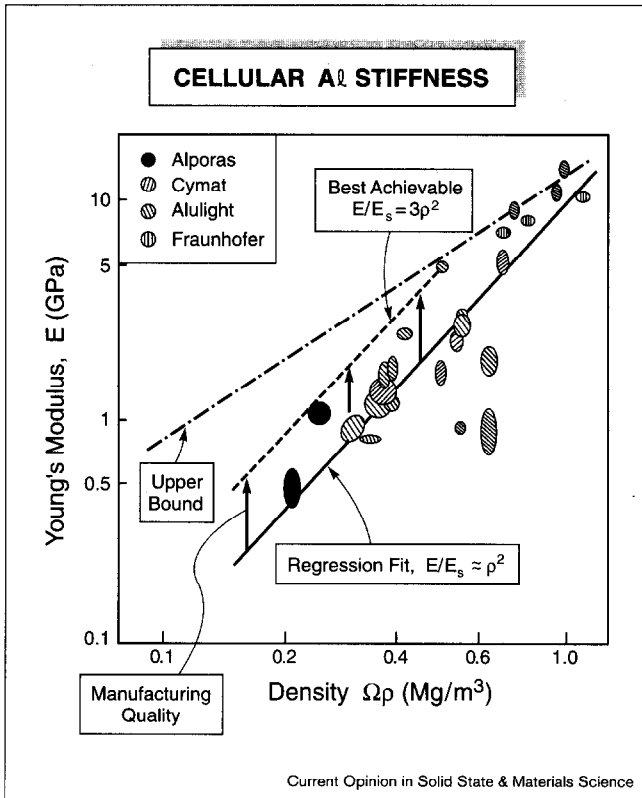
$$E/E_s = \alpha_1 \rho \qquad (1)$$

where E_S is the modulus of the solid material comprising the cell walls. The coefficient α_1 depends on the geometric arrangement of cells. For honeycombs, $\alpha_1 \approx 1$ for longitudinal loading, but only E is much lower for transverse loading [9]. For isotropic cells, elementary arguments suggest that, ideally, $\alpha_1 \approx 1/3$. Numerical results [15*,16,19,28] indicate magnitudes quite close to this elementary value. For tetrakaidecahedra, $\alpha_1 = 0.35$, with a weak dependence on the distribution of material between the borders and the walls [15*,16]. For thin-walled spheres, the stiffness is strongly affected by the radius of contact and the packing [19].

Open-cell solids, unless specially configured, are susceptible to bending, causing their stiffness to be relatively low and subject to the scaling [1*],

$$E/E_s = \alpha_2 \rho^2 \qquad (2)$$

where α_2 is approximately equal to unity.

Figure 2

Comparison of ideal and actual compressive mechanical properties for cellular Al materials: stiffness data for Al-alloys from the Cambridge Materials Selector (CMS) software [9].

Commercially available closed-cell metals have a stiffness lower than $\alpha_1 \sim 1/3$ in Equation 1 [9,15*,16-18]. The knockdown factors on α_1 are found to range from 2 to 50 (Figure 2). This knockdown effect arises because of morphological defects that induce bending and buckling deformations. The nature of these defects is elaborated in the section on 'Morphological defects'. Moreover, the totality of available data for closed-cell Al foams (Figure 2) is more comprehensively represented by Equation 2, rather than by Equation 1, with α_2 ranging from ~4 for the higher quality material to ~1/2 for inferior materials. This phenomenological scaling has utility in the analysis of minimum weight structures, as elaborated in the section on 'Minimum weight structures'.

Plastic flow

The inelastic properties of cellular metals have not been as extensively studied as their stiffness. Accordingly, the scaling relations remain to be substantiated. Numerical simulations indicate a negligibly small elastic region, because of localized yielding, followed by rapid strain hardening (even when the base material is perfectly plastic) and then a stress maximum. Equating the stress maximum to the yield strength, σ_0 (as defined in Figure 1) the available

theoretical results for closed-cell systems suggest a linear dependence on the density [1*,16,19,28] that is:

$$\sigma_0/\sigma_s = \alpha_3\rho \qquad (3)$$

where σ_S is the yield strength of the material comprising the cell borders. Results for the periodic tetrakaidecahedron, indicate that $\alpha_3 \approx 0.3$. But now, α_3 is significantly reduced upon distributing more of the material from the walls within the borders [15*].

The yielding of open-cell materials is limited by the bending stresses induced at the nodes, leading to the scaling:

$$\sigma_0/\sigma_s = \alpha_4\rho^{3/2} \qquad (4)$$

where the coefficient, $\alpha_4 \approx 0.3$ [1*].

Comparison with experimental measurements [9,16,18] requires independent information about the reference yield strength, σ_S. This yield strength has been estimated from microhardness measurements made on the cell walls. Based on such estimates of σ_S, and applying the definition of σ_0 given in Figure 1, the knockdown factor on α_3 for commercial closed cell Al-alloys is found to range from 4 to 100. It is the morphological defects as discussed in the relevant section of this review that are responsible.

Morphological defects

Most commercially available cellular metals, unlike some of their polymer counterparts, do not achieve the properties anticipated by Equations 1–4. The knockdown factor on these limits ranges from 2 to 100 [2*,15*,16-18] (Figure 2). Elimination of this knockdown, although not always important, can sometimes be crucial to the realization of performance advantages, particularly in strength-limited, lightweight structures (see the section on 'Minimum weight structures). Various hypotheses have been made regarding the 'defects' that diminish the properties [1*,2*,3,4*,5,6,7*,8-13,14*,15*,16-19,29,P1-P3]. These are now being systematically explored by combining both experimental and theoretical strategies, motivated by the potential to eliminate the most deleterious 'defects' through process control strategies.

There is an appreciable literature on the morphology and properties of liquid foams [28,30*,31,32]. This literature provides basic ideas and insights that establish the characteristics of 'ideal' foams, especially morphological factors. The differences between the morphologies found in cellular metals and liquid foams help establish some 'rules' that guide the thinking about 'defects'.

Morphological rules

The degrading effects of large bending moments and of low relative density suggest the following four 'rules' with respect to morphological defects:

1. Closed cellular structures that have straight walls and borders with uniform thickness should exhibit stiffnesses and strengths approaching the limiting values expressed by Equations 1 and 3 [16,19,28]. Accordingly, the presence of any features that depart from this rule might degrade the properties. In principle, many such features are possible and, indeed, are found in cellular metal structures [16–18]. They include: curved and wrinkled cell walls, thin or missing walls and high relative density domains (or inclusions). The challenge comprises the quantitative determination of the severity of these features. Progress towards this objective is addressed below.

2 The cell size distribution is not a dominant factor. Closed cell materials having essentially straight walls and equiaxed cells can have a relatively wide cell size range but still exhibit properties similar to those for materials with periodic, uniform cells [19,28]. This 'rule' provides a rationale for interpreting observations of morphological defects.

3. Defects that degrade the elastic properties must be present with a relatively high volume fraction, f. Composite theory dictates a knockdown factor on stiffness of the order, $(1-f)^{-1}$, indicating the need to emphasize only high volume fraction defects. Moreover, it highlights one of the problems in theoretical approaches for quantifying stiffness degrading defects. Namely, when introduced into cells with periodic boundary conditions, defects are necessarily present with high spatial frequency. Only by creating a model comprising many cells can the influence of defects with lower spatial frequency be explored.

4. Yielding initiates within small domains of spatially correlated defects. These correlated defects enable formation of a band of plastic deformation that spreads across the material [18].

Theoretical results

Performing theoretical work on morphological defects is challenging, especially for closed-cell materials. It is essential to use 3D models to include the membrane effect. However, it is restrictive to use periodic boundary conditions, because the effect of morphological defects is greatly exaggerated. Given the difficulty of a model that combines the 3D behavior with a sparse population of defects, the approach has been to gain insight from cell calculations. The eventual goal would be to introduce these result into an averaging scheme, in order to simulate the overall properties. Subject to these provisos, the following calculations have provided insight.

Calculations with periodic boundary conditions have illustrated two effects. Firstly, the distribution of material between the walls and the borders does not have an appreciable effect on the stiffness [19]. That is, upon thinning the walls (uniformly) and relocating the material at the nodes, the stiffness does not diminish until the walls become thin relative to the cell diameter. This insensitivity arises because bending effects are resisted by material placed at the nodes, thereby counteracting the reduction in membrane stiffness. Secondly, cell wall curves and wiggles cause dramatic reductions in stiffness and yield strength [16,19]. Their role in a nonperiodic structure remains to be quantified. Calculations in two dimensions with nonperiodic cells [29] have indicated that missing cell walls markedly diminish the yield strength. By inference, thin cell walls would have a similar effect.

Experimental measurements

The deformations of cells have been monitored using two principal methods: firstly, surface deformations by optical microscopy [21]; and secondly, internal cell deformations reconstructed by using X-ray computed tomography [18] (CT-scan).

Strain mapping methods [18] demonstrate that yielding is heterogeneous and occurs within bands about one cell diameter in width at stresses of the order of 1/3 of the plateau strength. Moreover, these bands intensify and their number density increases as the stress elevates, until a peak is reached. At the peak, plastic collapse occurs in one of the deformation bands. Each subsequent stress oscillation involves plastic collapse in successive bands.

X-ray results have been instrumental in establishing two salient aspects of yielding within the deformation bands [18]. In accordance with 'rules' 1 and 2, equiaxed cells resist yielding, almost regardless of their size. The corollary is that large cells, if equiaxed, are not the source of the knock-down factor. Consistent with 'rules' 1 and 4, elliptical cells with their long axis normal to the loading direction are prevalent within deformation bands, regardless of size. Such cells, in cross-section, typically have nodes with large entrained angles subject to appreciable bending moments. The inference is that cell ellipticity results in bending effects that reduce the yield strength. Accordingly, the following assertions are made about morphological defects: firstly, large equiaxed cells are relatively benign; secondly, cell ellipticity is detrimental, particularly for yielding; and thirdly, cell wall wiggles weaken the material.

Minimum weight structures
Structural indices

Panels, shells and tubes subject to bending or compression have characteristics determined by structural indices [3,4*,23–25]. These are obtained by deriving expressions for the stresses, displacements and weights in terms of the loads, dimensions, elastic properties and core densities. The details depend on the configuration, the loading and the potential failure modes. The book by Allen [33] provides an excellent basis for understanding the historical context and the methods of analysis. The indices are based on weight and load, they can be expressed either in non-dimensional form, (Ψ and Π, respectively, Table 1) or in convenient dimensional forms. The same indices apply

to bending or compression. For bending, it is convenient to define an additional structural index: the stiffness index, S. It is related to the elastic load index, Π_e, (Table 1) by: $S \equiv \Pi_e (L/\delta)$, where δ is the deflection, and L the span.

When optimizations are conducted simultaneously for weight and core density, explicit weight and deflection ratios result which, thereafter, greatly simplify determination of the relationships between the structural indices. For example, stiffness-limited, laterally-loaded panels containing a core with stiffness characterized by Equation 2 exhibit minimum weight when the face sheets weigh 1/4 that of the core. At this minimum, the contribution to the deflection by core shear is exactly twice that contributed by stretching the face sheet.

Table 1

Structural indices for foam core systems.

Indices	Column	Panel	Shell
Weight, Ψ	$W/\Omega L^3$	$W/\Omega L^2 B$	$W/\Omega R^2 L$
Load (elastic), Π_e	$P/E_f L^2$	$P/E_f LB$	$P/E_f LR$
Load (plastic), Π_p	$P/\sigma_y L^2$	$P/\sigma_y LB$	$P/\sigma_y LB$

B, width; E_f, Young's modulus of cellular material for face sheets; L, length of loaded structure; P, load; R, radius of shell; σ_y, yield strength of face sheets; Ω, density of cell wall material.

General considerations

The challenge is to establish prototypical structures and loadings that enable performance comparisons to be made. Broadly speaking, such comparisons indicate that sandwich construction is most likely to have performance benefits when the loads are in the elastic range, wherein the structure operates at design loads below those for face sheet yielding [4*; MY He, JW Hutchinson, unpublished data]. There are no benefits for designs based on limit loads, wherein the system squashes plastically. Subject to elastic behavior, a thin sandwich structure often has the lowest possible weight relative to competing concepts [4*; MY He, JW Hutchinson, unpublished data]. In some cases, the benefits are small. The implementation onus, therefore, is to find structures wherein the weight reductions are attractive over a sufficiently wide range of loads, as well as at practicable thicknesses and core densities to warrant their development.

Without accounting for multiple failure modes, it is not possible to determine minimum weights of sandwich configurations when the properties scale linearly with relative density. In consequence, the results for open cell materials are used (Equations 2 and 4), but using coefficients α_2 and α_4 that encompass the property ranges measured experimentally.

Stiffness-limited applications

Panels that experience lateral loads are often stiffness limited. Stiffness also affects the natural vibration frequencies [2*]. That is, high stiffness at low weight increases the resonant frequencies, thereby facilitating their avoidance in application.

Choosing minimum weight configurations is relatively straightforward whenever the design loads allow choices entirely within the elastic range: that is, no yielding of either the face sheets or the core. The basic concepts can be found in several literature sources [1*,33]. The key results are repeated here to establish the procedure as well as the most useful results. For all bending problems, a series of non-dimensional coefficients, (designated A_1 to A_4) relate the deflections to the moments. These have been comprehensively summarized in the Ashby Design Guide [9,2*,34] and they will be used throughout the following derivations.

Two ratios arising from minimization are the essential starting point. Reiterating, the displacements contributed by core shear are twice those from bending moments and the core weight is four times that of the face sheets. The non-dimensional relationship derived from these weight ratios that connects stiffness, weight and core thicknesses, c, is:

$$S = (A_1/60)(c/L)^2 \Psi \tag{5}$$

In deriving this expression it has been assumed that the core and face sheets are made from the same materials $(E_f = E_s, \Omega = \Omega_f)$. At the minimum, the core thickness is explicitly related to the stiffness by:

$$\frac{c}{L} = 2\left[\frac{18\alpha_2 A_2 S}{A_1^2}\right]^{1/5} \tag{6}$$

Substituting c/L into Equation 5 gives the interrelationship:

$$\Psi = \frac{15S^{3/5}}{A_1^{1/5}(18\alpha_2 A_2)^{2/5}} \tag{7}$$

For plotting purposes, it is convenient to re-express Equation 7 in the form
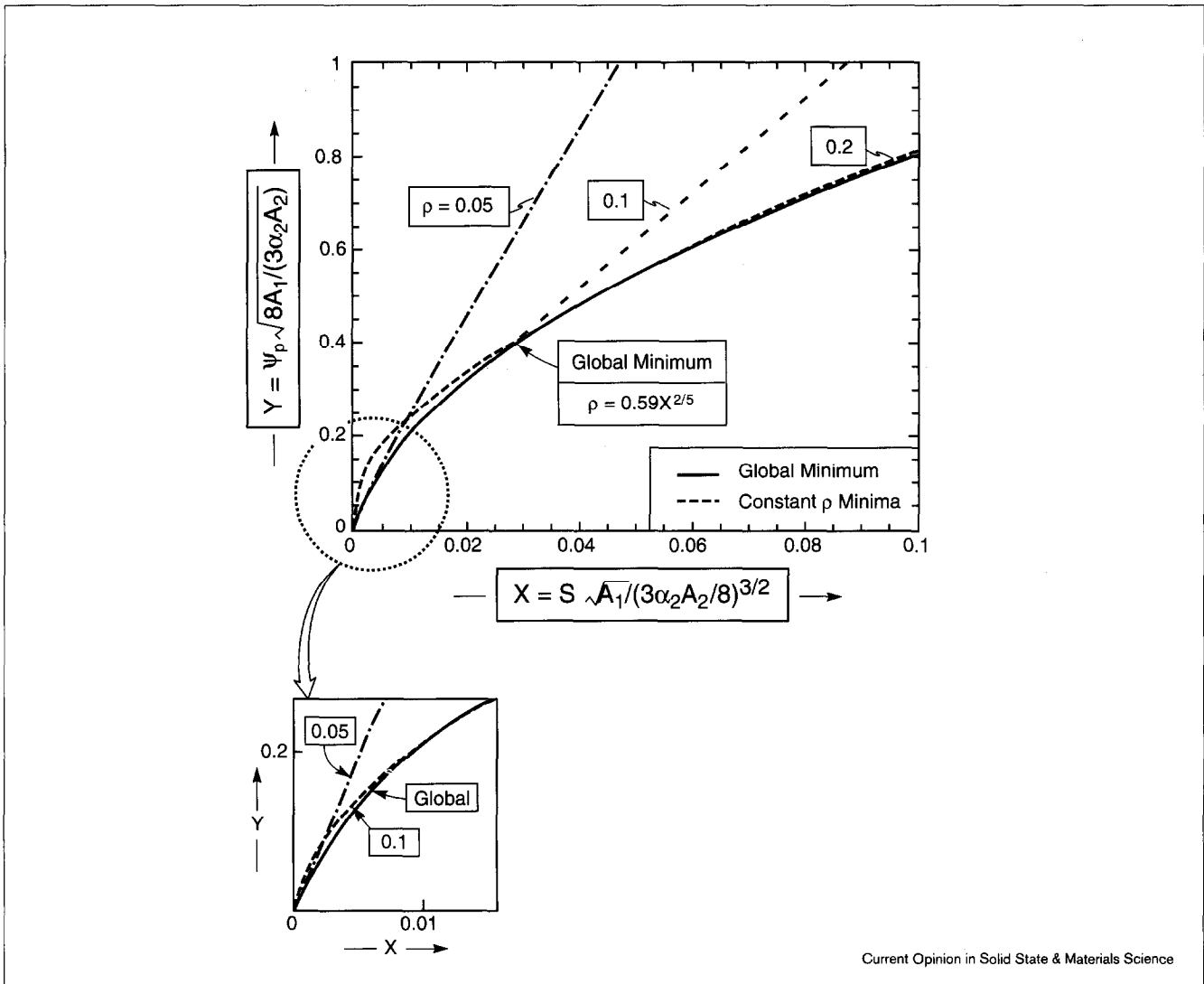
$$Y = 3.19X^{3/5} \tag{8}$$

where

$$Y = \Psi = \sqrt{8A_1 / 3\alpha_2 A_2} \tag{9a}$$

and

$$X = S = \sqrt{A_1/3\alpha_2 A_2/8)^{3/2}} \tag{9b}$$

This result is plotted on Figure 3.

Figure 3

Minimum weight analysis for stiffness-limited, laterally loaded panels. A cross plot of the minimum weight and stiffness indices showing the global minimum, as well as minima for three fixed densities (ρ_c/ρ_S = 0.05, 0.1 and 0.2). Note that, for the global minimum, the core density is given by, $\rho_c/\rho_S = 0.59 X^{2/5}$.

For each stiffness, there is a corresponding optimum in the relative density:

$$\rho = 0.59 X^{2/5} \qquad (10)$$

There is also an explicit face thickness,

$$\frac{d_f}{L} = \frac{A_1}{96 \alpha_2 A_2} \left(\frac{c}{L} \right)^3 \qquad (11)$$

In some cases, it is more realistic to consider sandwich panels having weight minimized with respect to skin and core thicknesses at specific core density. Then, for each density, a cross-plot of stiffness and weight indices can be superimposed onto Figure 3. The results are expressed as a relationship between Y and X with ρ as a parameter. The solutions for three choices of ρ are plotted in Figure 3. Each makes contact with the global minimum at a single point where its core density coincides with that of the globally minimized sandwich. Note that, for high stiffness requirements, the weights of sandwiches with a relative core density, ρ = 0.2, are only slightly larger than the global minimum over a substantial range about the point of coincidence. At lower stiffnesses, this design becomes significantly heavier and much lower core densities are needed to realize the global weight minimum.

Application of these weight diagrams is limited by the occurrence of yielding, either of the face sheets or in the

core, and by face wrinkling. Face yielding commences when the maximum tensile or compressive stress caused by bending reaches the tensile yield strength, σ_Y. For the globally optimal sandwich, this result can be expressed in terms of X:

$$Z_f \gtrless X^{4/5} \tag{12}$$

where Z_f is given by:

$$Z_f = \left(\frac{P}{BL\sigma_Y}\right)\left[\frac{16A_1}{48^{4/5}\alpha_2 A_2 A_3}\right]$$

For a given transverse load, P, all globally optimized designs less stiff than that associated with the equality in Equation 12 exceed yield in the face sheets. That is, configurations having lower stiffness cannot be realized at the weights given by Equation 12. Weights in excess of the global minimum would be needed to obtain stiffnesses in this range.

For the optimally designed sandwich, core yielding occurs when:

$$Z_C \gtrless X^{1/5} \tag{13}$$

$$\text{where } Z_C = \left(\frac{P}{BL\tau_c}\right)\sqrt{\frac{A_1}{\alpha_2 A_2}}\left[\frac{1}{48^{1/5}A_4}\right],$$

with a similar interpretation to that for face yielding. Here τ_c is the shear yield strength for the core. Again lower stiffnesses cannot be realized at the global weight minimum, this time because of core yielding.

The global weight minimum prevails, perhaps surprisingly, when structural requirements dictate high stiffness. This result arises because the face sheet thicknesses needed to achieve minimum weights increase substantially as the stiffness index increases, relative to core thickness and density [2*]. At lower stiffnesses, because of the thinner face sheets and lower core densities at the global weight minimum, yielding is more likely to intercede. For yielding to be avoided, the loads on the structure must by limited by Equations 10b and 10c. Alternatively, the weight may be increased above the minimum by increasing either the face sheet thickness or the core density.

Competing concepts

Competition for sandwich panels is comprised principally of waffle-stiffened panels. For comparison, it is convenient to re-express Equation 7 in the form:

$$\frac{W}{BL^2} = \Omega\left(\frac{P/\delta}{BE_f}\right)^{3/5}\left[\frac{15}{A_1^{1/5}(18\alpha_2 A_2)^{2/5}}\right] \tag{14}$$

For a waffle panel subject to bending about one of the stiffener directions, the weight and stiffness are interrelated by:

$$\frac{W}{BL^2} = \frac{72}{5}\left(\frac{P/\delta}{E_o A_1 B}\right)\left(\frac{L}{d_s}\right)^2 \tag{15}$$

where d_S is the stiffener depth, with E_o Young's modulus for the material comprising the panel and Ω_o its density. Equating the weights of the sandwich and waffle panels, Equations 14 and 15 give:

$$\frac{d_s}{L} = \sqrt{\frac{72}{125}\left(\frac{\Omega_o}{\Omega}\right)\left(\frac{E_f}{E_o}\right)}\left(\frac{P/\delta}{BE_f}\right)^{1/5}\left(\frac{18\alpha_2 A_2}{A_1^2}\right)^{1/5} \tag{16}$$

Comparison with the optimized sandwich panel yields, at equivalent weight:

$$\frac{d_s}{c} = \frac{\sqrt{6}}{5}\sqrt{\left(\frac{\Omega_o}{\Omega}\right)\left(\frac{E_f}{E_o}\right)} \tag{17}$$
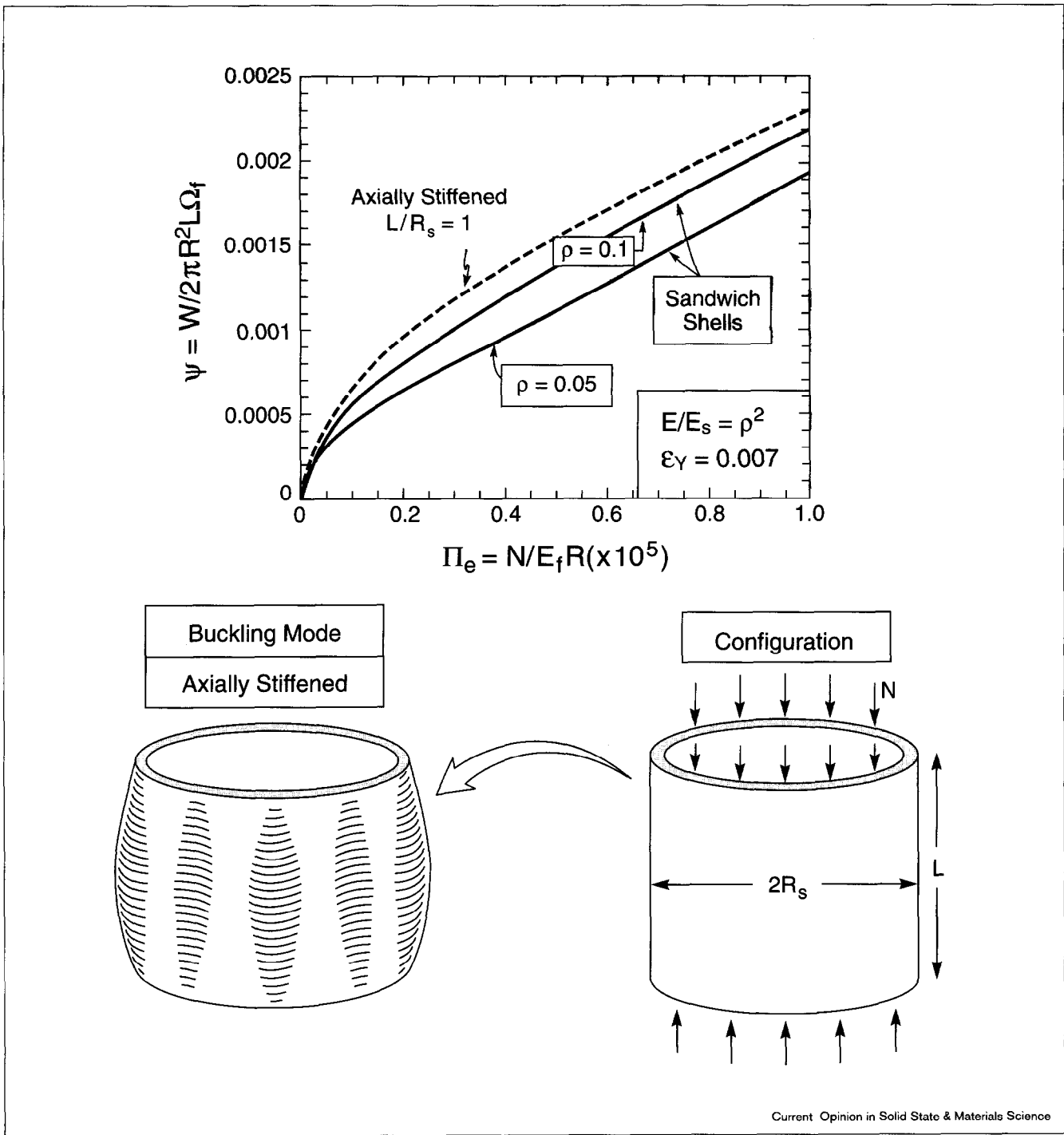
This result is stiffness independent because Equations 6 and 16 have the identical functional dependence. Accordingly, a waffle panel made from the same material as a sandwich panel ($\Omega = \Omega_o$, $E_f = E_o$) has a slightly smaller overall thickness, at the same weight and stiffness. The choice, therefore, depends entirely on manufacturing cost and durability.

Axially compressed shells

Minimum weight requirements for strength-limited structures are illustrated using cylindrical sandwich shells subject to axial compression. These can be weight competitive with stiffener reinforced shells: the lowest weight designs in current usage. Moreover, shells are a more likely candidate for sandwich construction than axially compressed panels. This preference arises because both hoop and axial stresses are involved, enabling the isotropy of sandwich panels to be exploited. Conversely, in panels, only axial stresses arise: a situation wherein unidirectional stiffeners are especially efficient. There are two basic requirements for sandwich shells. Sufficient core shear stiffness is needed for adequate buckling strength and the shear yield strength of the metal foam must be large enough to maintain the buckling resistance of the shell, particularly in the presence of imperfections.

Two examples of minimum weight, perfect sandwich cylinders are summarized in Figure 4. These shells have been optimized with respect to d_f (face sheet thickness) and c, subject to prescribed core density [35,36; MY He, JW Hutchinson, unpublished data]. These examples regard the fully dense core material as identical to the face sheet material ($\Omega_f = \Omega$, and $E_f = E_S$), and use a core with stiffness at the low end of the range found for commercial materials

Figure 4

Minimum weight comparisons for strength-limited, axially compressed cylindrical sandwich shells at fixed density (with $\alpha_2 = 1$) having dimension $l/R = 1$, compared with those for a shell with inside stiffeners.

($\alpha_2 = 1$). The face sheets are elastic-perfectly plastic with compressive yield strength σ_Y. Note that, at the optimum weight, and in the range where the face sheets experience yield, the compressive stress in the face sheets associated with elastic buckling is coincident with the yield strength in compression, σ_Y (MY He, JW Hutchinson, unpublished data). The weight index has been determined at a representative yield strain for Al alloys ($\varepsilon_Y = 0.007$). These results are independent of the length of the cylinder. The buckling mode is indicated in the inset.

Included in Figure 4 is the structural performance calculated for an optimally-designed, axially-stiffened cylindrical shell with hat-shaped stiffeners located on the inside. These results apply to a shell segment located between rings spaced a distance L apart, with $L/R = 1$. A lower L/R would have a lower weight index, and vice versa. Note that, over the range plotted, the shell buckles elastically for the chosen yield strain. (Shells with stiffeners on the outside of the cylinder have somewhat greater buckling strength and, thus, a lower weight index. But, outside stiffening is often excluded for other reasons.) "This example illustrates that metal foam core sandwich shells can have a competitive advantage over established structural methods of stiffening, particularly at relatively low structural indices."

Other configurations

Results for minimum weight sandwich panels at a fixed cored density, $\rho = 0.1$ are not especially promising [4*]. There is only a small domain of weight savings. This domain arises when sandwich construction is used within the stringers, as well as the panels, of a stringer-stiffened configuration. This construction has lowest weight at small levels of load index. Further minimization with core density leads to more pronounced weight savings. In this case, even flat sandwich panels can weigh less than stringer-stiffened panels, especially at lower levels of load index. The challenge in taking advantage of the potential weight savings arises in manufacturing.

Results for columns indicate that thin-walled sandwich tubes are lighter than foam filled and conventional tubes, but the beneficial load ranges are small [4*].

Thermal management: heat transfer media

Thermal conductivities of metal foams are at least an order of magnitude greater than their nonmetallic counterparts, so they are generally unsuited for thermal insulation. Open-cell metal foams, however, can be used to enhance heat transfer in applications such as cryogenic heat-exchangers, heat-exchangers for airborne equipment, compact heat-sinks for power electronics, heat-shields, air-cooled condenser towers and regenerators. The heat transfer characteristics of open-cell metal foams are summarized on the following pages.

Heat transfer coefficient

The cellular metallic medium can be characterized by a heat transfer coefficient, H_c [6,7*] given by:

$$H_{\mathrm{c}} = \frac{2\rho}{d} k_{eff} \sqrt{Bi_{eff}} \tanh\left[\frac{2b}{d}\sqrt{Bi_{eff}}\right] \qquad (18)$$

Here k_{eff} is an effective thermal conductivity related to the actual thermal conductivity of the constituent metal, k, by:

$$k_{eff} = \lambda_1 k \qquad (19)$$

with $\lambda_1 = 0.28$ being a proportionality constant calibrated by experiment [13]; b, the thickness of the medium (Figure 5), ρ the relative density and d the diameter of the metal ligaments. Bi_{eff} is an effective Biot number, which relates to that for a staggered bank of cylinders, Bi, by:

$$Bi_{eff} = (\lambda_2/\lambda_1)Bi \qquad (20)$$

with $\lambda_2 = 0.34$ being another proportionality constant [13] and

$$Bi \equiv h/dk \qquad (21)$$

with h the local heat transfer coefficient between the metal ligaments and the flowing fluid.

The Biot number is governed by the dynamics of fluid flow in the cellular medium. By using the effective value (Equation 20), it can be connected with established solutions for a staggered bank of cylinders:

$$\begin{aligned} Bi &= 0.914 Pr^{0.36} Re^{0.4}(k_a/k) \ (Re \leq 40) \\ &= 0.625 Pr^{0.36} Re^{0.5}(k_a/k) \ (Re > 40) \end{aligned} \qquad (22)$$

where the Reynolds number is

$$Re = vd/v_a \qquad (23)$$

with v the free stream velocity of the fluid, v_a its kinematic viscosity, k_a its thermal conductivity and Pr the Prandtl number (of order unity) [37–39].

This set of equations provides a complete characterization of the heat transfer coefficient. The trends are found upon introducing the properties of the foam (d, ρ and k), its thickness b, and the fluid properties (v_a, k_a and Pr), as well as its velocity, v. The proviso is that the proportionality constants (λ_1 and λ_2) have only been calibrated for one category of open-cell foam: the ERG range of materials. Open-cell foams having different morphology are expected to have different λs. Moreover, if ρ and d are vastly different from the values used in the calibration, new domains of fluid dynamics may arise, resulting again in deviations from the predictions.

The substrate attached to the cellular medium also contributes to the heat transfer. In the absence of a significant thermal constriction, this contribution may be added to H_c (Equation 18), such that the overall heat transfer coefficient, H_o, is:
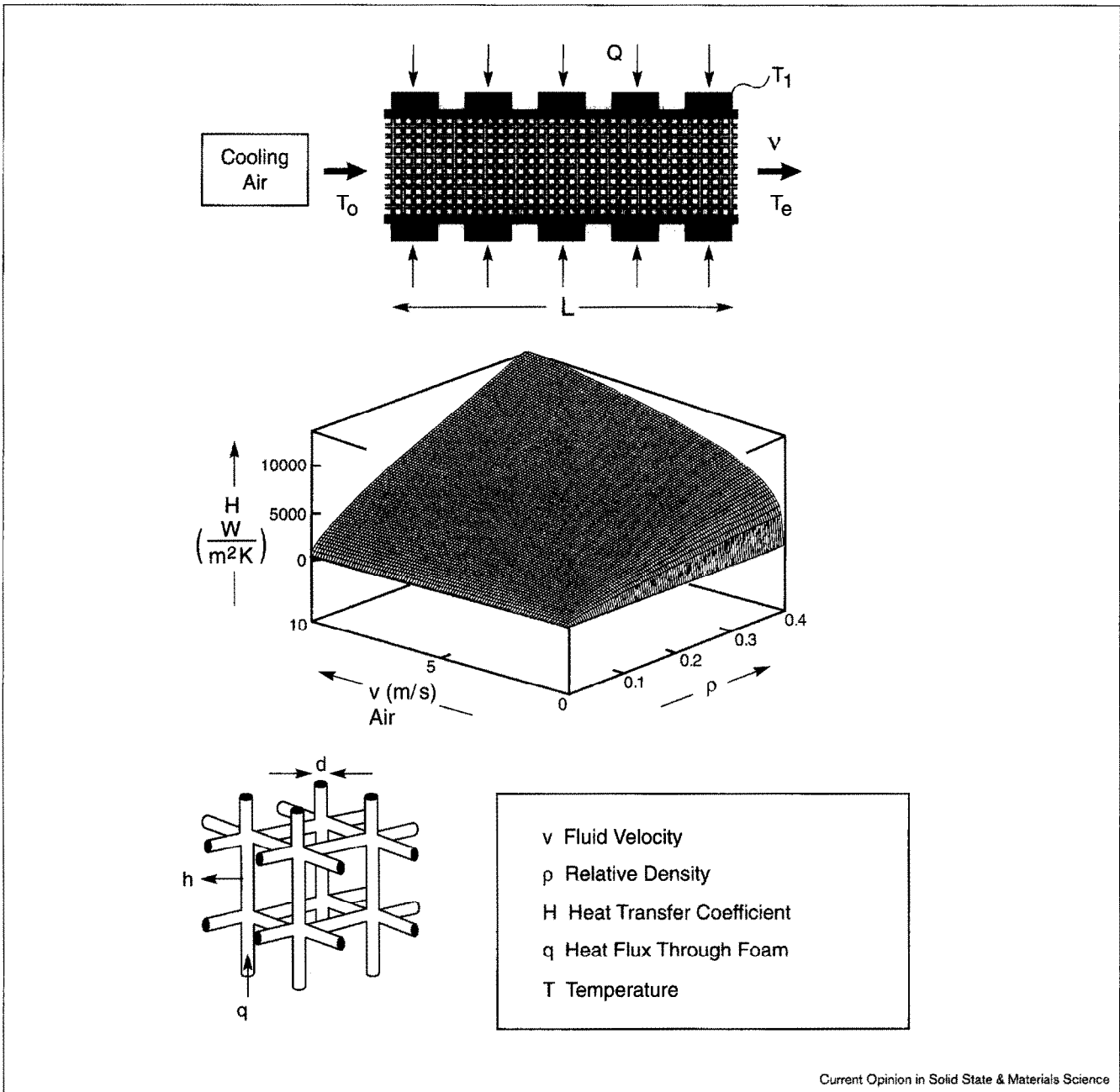
$$H_o \approx H_c + \eta Bi_{eff} k_{eff} \qquad (24)$$

where

$$\eta = 1 - 0.22\rho$$

More typically, there are interface effects that reduce H_o.

Figure 5

A schematic of an open cell metal used as a heat dissipation medium, for example, for cooling high power electronics. Also shown is the heat transfer coefficient calculated for the system as a function of the fluid velocity and the relative density of the foam, upon geomtetrically representing the foam as a bank of cylinders shown in the inset. L, length of loaded structure; Q, heat flowing into the fluid; T_e, fluid temperature at the outlet; T_o, fluid temperature at the inlet; T_1, temperature of the heat source.

Heat fluxes

The heat Q flowing into the fluid through the cellular medium per unit width is related to the heat transfer coefficient by:
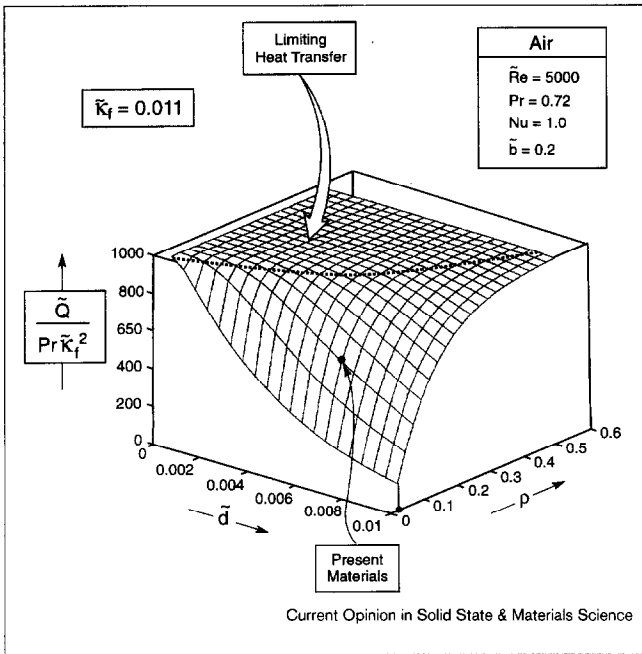
$$Q = LH_o\Delta T_{lm} \tag{25}$$

where L is the length of the medium (Figure 5) [37–39].

Here ΔT_{lm} is the logarithmic mean temperature. It is related to the temperature of the heat source T_1, as well as to the fluid temperature at the inlet, T_o and that at the outlet, T_e by:
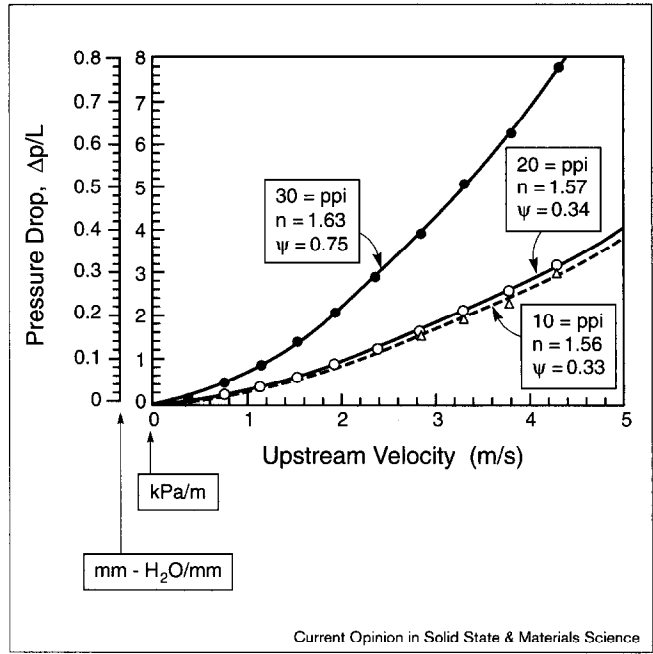
$$\Delta T_{lm} = \frac{T_e - T_o}{\ell n\left[(T_1 - T_o)/(T_1 - T_e)\right]} \tag{26}$$

Figure 6

Predicted heat dissipation as a function of cell wall diameter and relative density for cellular Al-alloys [6]. A full description of the non-dimensional quantities, $\tilde{Q}$, $\tilde{d}$, $\tilde{\kappa}_f$ and $\tilde{b}$ can be found in [6].

Figure 7

The pressure drop measured for three commercially available open cell Al materials, all made by ERG [9]. ppi, pores per inch; ψ, weight index.

Usually, T_1 and T_o are specified by the application. Accordingly, T_e must be assessed in order to determine Q. For preliminary estimates, the approximation

$$\Delta T_{lm} \approx T_1 - T_o \tag{27}$$

may be used. Explicit determination requires either experimental measurements or application of the following expressions governing the fluid flows.

The temperature in the fluid along the flow-direction varies as ($T_f < T_{metal}$) [6,7•],

$$T_f = T_1 - (T_1 - T_o)\exp(-x/l) \tag{28}$$

where l is a transfer length governed by the properties of the cellular metal, the fluid and the substrate. In the absence of a thermal resistance at the attachments, this length is:

$$\ell = \frac{\rho_a c_p b v}{2\eta k_{eff}\sqrt{Bi_{eff}}}\left[1+\frac{\rho}{1.5\eta}\tanh\left(\frac{2b}{d}\sqrt{Bi_{eff}}\right)\right]^{-1} \tag{29}$$

where c_p is the specific heat of the fluid [6,7•].

The exit temperature may thus be determined by introducing l from Equation 29 into Equation 28 and setting $X = L$. Then, Q is explicitly defined in terms of ($T_1 - T_o$). A

surface showing how Q depends on relative density ρ and ligament size d is presented in Figure 6 [6]. Definitions of the non-dimensional terms can be found in [6].

Pressure drop

As the heat transfer coefficient increases, the pressure drop across the medium also increases. The latter can sometimes be the limiting factor in application, because of the available pumping power. The pressure drop Δp has the general form:

$$\Delta p / L = \xi(1/a)\left[v_a^m \rho_a /(1-\alpha)^{2-m}\right]v^{2-m}d^{-m} \tag{30}$$
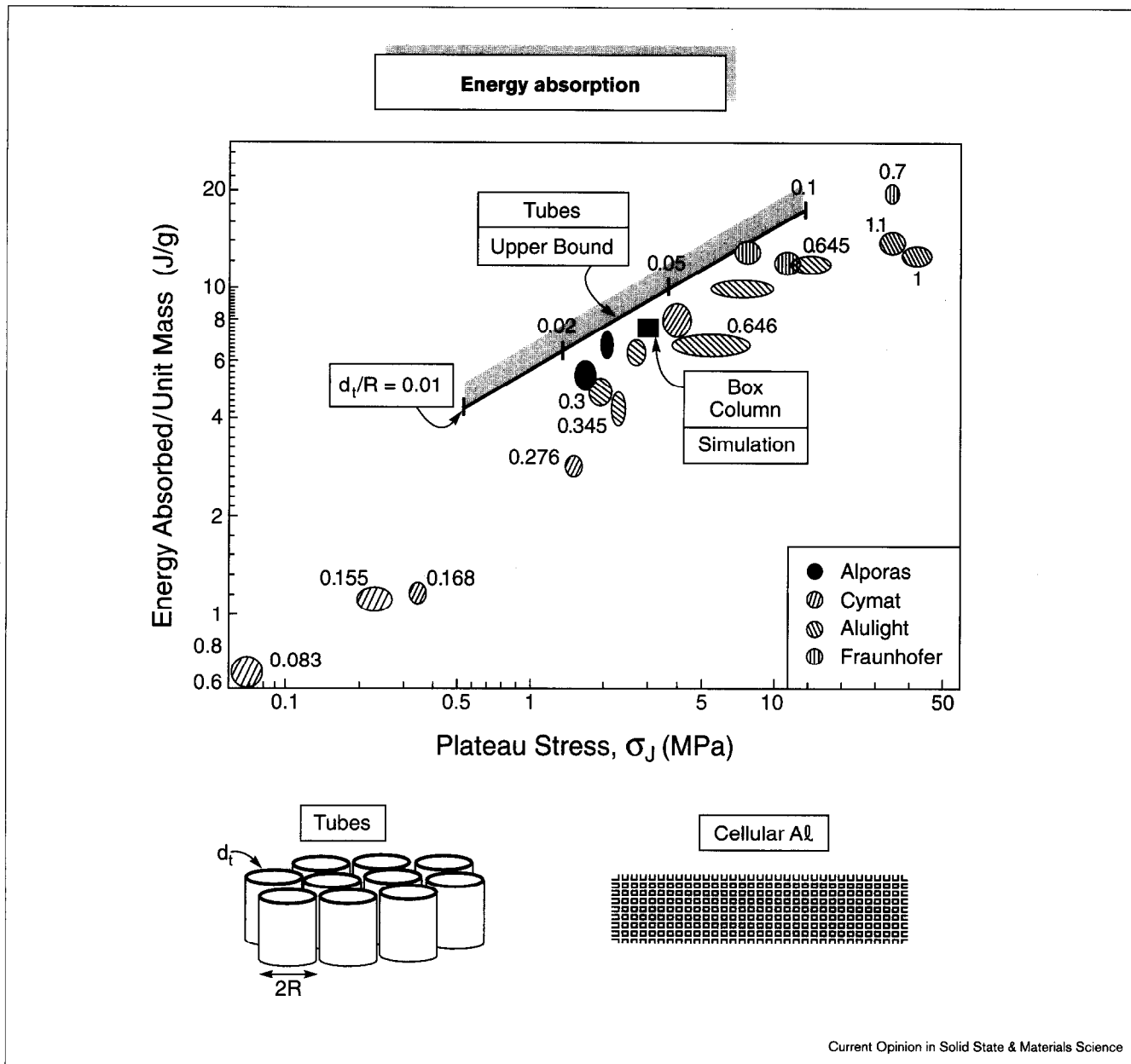
where a is the cell size,

$$a = 1.24d\sqrt{3\pi/\rho} \tag{31}$$

The exponent m and the coefficient ξ have been calibrated by experimental measurements [6]. They are:

$$m = 0.4 \tag{32}$$
$$\xi = 4$$

Some typical results are plotted in Figure 7. Pressure drops for other conditions can be predicted from Equations 30–32, again with the proviso that the fluid flow scaling in Equation 23 retains its validity.

Figure 8

Energy absorption

A comparison of the energy absorption per unit mass for Al foams and tubes.

Energy absorption

Metrics

A comprehensive treatment of energy absorption by foams has been given by Gibson and Ashby [1•]. A few salient results are repeated here for completeness. The compaction strain, ε_d (Figure 1), is dictated solely by the relative density [1•], such that:

$$\varepsilon_d = 1 - \rho\phi_v \qquad (33)$$

where ϕ_v is a measure of the relative void space retained when the cells have collapsed: it is ~1.4. The energy absorption per unit volume, U, is:

$$U/\sigma_J = \varepsilon_d \qquad (34)$$

Accordingly, a plot of U against σ_J is dictated by the densification strain (Figure 8a), causing all data for cellular Al-alloys to reside along a diagonal band. The corresponding result for the energy absorbed per unit mass, U_p, is:

$$\begin{aligned} U_p / \sigma_J &= \varepsilon_d / \rho\Omega \\ &\equiv \frac{(1 - \rho\phi_v)}{\rho\Omega} \end{aligned} \qquad (35)$$

A plot of U_p against σ_J now has an additional dependence on density. But, as σ_J also depends on density (see Equation 3), the data for cellular Al-alloys still reside within a relatively narrow band (Figure 8), with less than a factor of two spread in energy adsorption among the better quality commercial materials. Specifically, upon using Equation 3 as representative of σ_J for closed-cell materials, the realizable energy absorption becomes

$$U_p / \sigma_s = \alpha_3(1-\rho\phi_v) / \Omega \qquad (36)$$

The energy absorption can only be appreciably increased by elevating the plateau stress. Accordingly, when the allowable stress is specified by the application, the energy is largely 'predetermined by the inherent deformation characteristics of the material'. The only significant materials issue concerns the ability to adjust the stress. Accordingly, for energy absorption purposes, 'there is minimal motivation for manufacturing developments that enhance the morphological quality beyond that achievable in the better commercially available materials'.

Upon impact, kinetic energy $\kappa(=mv^2/2)$ from the object must be dissipated by plastic work. The impact can be fully absorbed without exceeding the stress, σ_J, if the foam thickness, D, satisfies:

$$D \gtrless \kappa/UA_I \qquad (37)$$

where A_I is the area over which the impact is spread by interaction with the buffer plate. The minimum weight of cellular material ,W_{min}, needed to absorb the impact is:

$$W_{min} = \kappa/U_\rho \qquad (38)$$

System comparison

Competition for cellular materials is provided by banks of either thin-walled or annular sandwich columns. In columnar configurations, the energy is absorbed through plastic buckling of the walls. The collapse of tubes and their energy absorption have been analyzed [40,41]. The energy absorbed per unit volume is found to be:

$$U/\sigma_s \equiv \sigma_f\varepsilon_d \qquad (39)$$
$$= 2^{1/2}\rho^{5/3}(1 - \rho)$$

The corresponding energy per unit mass is

$$U_p/\sigma_s = 2^{1/2}\rho^{2/3}(1 - \rho)/\Omega \qquad (40)$$

As Al tubes can be made with yield strength, $\sigma_S \approx 200$ MPa, the energy absorptions can be superposed onto the cellular Al data for comparison purposes (Figure 8). The comparison suggests that Al-alloy tubes are superior to cellular alloys on a weight basis. However, two additional considerations enable the cellular materials to be competitive in some cases. Firstly, numerical simulations of column

crushing [5] indicate stress oscillations as plastic buckling progresses, resulting in energy levels about 2/3 those expected from Equation 40. Secondly, tubes absorb efficiently only upon axial loading; they are much less effective when impacted obliquely. Cellular media are isotropic and omnidirectional. Accordingly, when impacts from a range of directions are expected, foams are attractive.

Conclusions

The connections between the morphological quality of cellular metals and the requirements for their implementation comprise: firstly, those insensitive to the thermomechanical properties of the material and secondly, others that are strongly influenced by cellular material quality. This distinction partitions the connection between manufacturing and implementation.

Several applications categories are insensitive to morphological quality, provided that some reasonable minimum is consistently achieved. These comprise energy absorption applications and some ultralight panels and tubes. The latter category includes some stiffness limited structures, as well as strength limited configurations subject to low imperfection sensitivity.

Other applications categories require that the cellular material have the best achievable thermomechanical properties. One category comprises imperfection sensitive ultralight shells and circular tubes that operate in the elastic range. In such cases relatively high strength cores, approaching the best achievable, are essential to the realization of substantial weight savings. Another category comprises open cell heat dissipation media.

Within these overall material property benchmarks, comparisons with competing materials and systems suggest the following three implementation opportunities.

Firstly, for heat dissipation purposes, cellular metals are unique. Moreover, there are substantial opportunities to greatly improve their thermal performance by tailoring cell size and density. The manufacturing challenge is demanding, but justified by the performance benefit.

Secondly, cellular Al-alloys are attractive in those applications that require exceptional energy absorption: yet, are compatible with moderately high stress delivery levels (1–10 MPa). Manufacturing requirements are not especially stringent for these applications, enabling the use of lower cost process methods. The isotropy of the foams and the uniformity of their force delivery represent performance advantages over competing concepts, such as thin walled box columns.

Thirdly, strength and stiffness limited ultralight structures designed within the elastic range all exhibit a domain wherein weight benefits arise from the use of thin sandwich construction comprising cellular metal cores. Only a

subset of these structures have sufficient performance benefit to justify implementation. Preliminary attempts at defining these structures have identified panels and shells as opportunities. The greatest benefits appear to arise with relatively long strength-limited shells subject to axial compression. There also appear to be opportunities for stiffness limited panels that experience lateral loads. There are no benefits for compression structures designed with a load index in the plastic range. The requirements on the mechanical properties of the cellular material are themselves subject to the imperfection sensitivity of the structure. For imperfection insensitive structures, the dictation on properties are minimal. But, the benefits from using a cellular core are also small. Conversely, imperfection sensitive structures, such as cylindrical shells, benefit most from having cellular cores with properties approaching the best achievable levels, with no knockdown. Cellular metal sandwich construction would provide even greater weight benefit if the density of the core could be substantially decreased below that of presently available materials, subject to mechanical properties that approach best achievable levels (Equations 1 and 3). Attainment of such materials constitutes a longer range manufacturing objective.

References and recommended reading

Papers of particular interest, published within the annual period of review, have been highlighted as:

- of special interest
- • of outstanding interest

1. Gibson LJ, Ashby MF: *Cellular Solids, 2nd Edn.* Cambridge, UK:
•   Cambridge University Press; 1997.
This is the 'bible' of cellular solids. It is essential reading to anyone seriously interested in this topic.

2. Ashby MF, Hutchinson JW, Evans AG: *Cellular Metals, A Design*
•   *Guide.* Cambridge, UK: Cambridge University, Engineering Department; 1998, in press.
When issued, this will be a user friendly, more complete version of the present review having special relevance to designers wishing to use cellular metals.

3. Shanley FR: *Weight-Strength Analysis of Aircraft Structures.* New York: Dover; 1960.

4. Budiansky B: **Harvard university report, mech 319 (1997).** *Int J*
•   *Solids Structures* 1998, in press.
This new paper has a unique set of results comparing sandwich configurations with conventionally stiffened structures in buckling limited systems. It gives key insights into the important issues governing minimum weight designs.

5. Santosa SP, Wierzbicki T: *Computers & Structures* 1998, in press.

6. Bastawros A, Stone HA, Evans AG: *J Heat Transfer* 1998, in press.

7. Lu TJ, Stone HA, Ashby MF: *Acta Mater* 1998, in press.
•   This is a key paper describing theoretical relationships between heat flux, pressure drop and foam properties. Subsequent experimental studies have validated the ideas, albeit with two effective properties to take account of the greater morphological complexity of a cellular materials relative to a bank of cylinders.

8. Beals JT, Thompson MS: **Density gradient effects on aluminium foam compression behaviour.** *J Mater Sci* 1997, **32**:3595-3600.

9. Ashby MF, Seymour CJ, Cebon D: *Metal Foams and Honeycombs Database.* Granta Design; 1997.

10. Davies GJ, Zhen S: **Metallic foams: their production, properties and applications.** *J Mater Sci* 1983, **18**:1899-1911.

11. Thornton PH, Magee CL: **Deformation characterisation of zinc foams.** *Metall Trans* A 1975, **6**:1801-1828.

12. Martin RL, Lederich BJ: In *Advances in Powder Metallurgy. Powder Metallurgy Conference and Exhibition: Chicago, IL.* Princeton, NJ: The Metal Powder Industries Federation; 1991:361-370.

13. Kearns MW, Blenkinsop PA, Barber AC, Farthing TW: **Manufacture of a novel porous material.** *Int J Powd Met* 1988, **24**:59-64.

14. Nagel AR, Hurysz KM, Lee KJ, Cochran JK, Sanders TH Jr: **Closed**
•   **cell steel foams: fabrication and mechanical testing.** Atlanta, GA: Georgia Institute of Technology, School of Material Science and Engineering; 1998.
This paper describes an innovative way for making high quality hollow metal spheres that can be later consolidated into a cellular material.

15 Simone AE, Gibson LJ: **Effects of solid distribution on the stiffness**
•   **and strength of metallic foams.** *Acta Mater* 1998, **46**:2139-2150.
Sophisticated numerical models that characterize the role of morphological defects on the elasticity and yielding of cellular metals.

16. Simone AE, Gibson LJ: **Efficient structural components using porous metals.** *Acta Mater* 1998, **46**:55-62.

17. Sugimura Y, Meyer J, He MY, Bart-Smith H, Grenestedt JL, Evans AG: **On the mechanical performance of closed cell Al alloy foams.** *Acta Mater* 1997, **45**:5345-5359.

18. Bart-Smith H, Bastawros AF, Mumm DR, Evans AG, Sypeck DJ, Wadley HNG: **Harvard university, mech-313.** *Acta Mater* 1998, in press.

19. Grenestedt JL: *J Mech Phys Solids* 1998, **46**:29-50.

20. Ultralight Metal Structures, Annual Report 1996/1997. The Defense Advanced Research Project Agency and the Office of Naval Research; 1997.

21. *Proceedings of the International Conference on Metal Foams and Porous Metal Structures: 1998 July 11–13; Bremen, Germany.* Chairmen, Banhart J, Ashby MF, Fleck N.

22. On the World Wide Web: Muri Web Page access information: http://daswww.harvard.edu/users/faculty/Anthony_Evans/Ultralight_Conference/UltralightStructures.html

23. Farrar DJ: *J Royal Aeronautical Soc* 1949, **53**:1041-1052.

24. Gerard G: *Minimum Weight Analysis of Compression Structures.* New York: New York University Press; 1956.

25 Thompson JMT, Lewis GM: *J Mech Phys Solids* 1972, **20**:101-109.

26. *Aeronautical Technology for the Twenty-First Century.* National Academy Press; 1992.

27. Renaud M, Giamei A, Priluck J: *Materials Research Society Proceedings* 1998, in press.

28. Kraynik AM, Reinelt DA: **Linear elastic beavior of dry soap foams.** *J Colloid Interface Sci* 1996, **181**:511-520.

29. Silva MJ, Gibson LJ: **The effects of non-periodic microstructure and defects on the compressive strength of two-dimensional cellular solids.** *Int J Mech Sci* 1997, **39**:549-563.

30. Kraynik AM, Neilsen MK, Reinelt DA, Warren WE: *Proceedings of the*
•   *NATO Advanced Study Institute on 'Foams, Emulsions, and Cellular Materials: 1997 May 11–24; Cargese, Corsica.* Edited by Sadoc J, Rivier N. Amsterdam: Kluwer; 1997
This is a major review of foam morphologies and their deformation characteristics.

31. Weaire D, Fortes MA: **Stress and strain in liquid and solid foams.** *Adv Phys* 1994, **43**:685-738.

32. Kraynik AM, Reinelt DA: *Forma* 1996, **11**:255-270.

33. Allen HG: *Analysis and Design of Structural Sandwich Panels.* Oxford: Pergamon; 1969.

34. Ashby MF: *Materials Selection for Mechanical Design.* Oxford: Pergamon; 1989.

35. *Buckling of Thin-walled Circular Cylinders,* NASA SP-8007 1965. [Revised 1968].

36. Sullins RT, Smith GW, Spier EE: *Manual for Structural Stability Analysis of Sandwich Plates and Shells.* NASA-CR-1457; 1969.

37. Bejan A: *Heat Transfer.* New York: John Wiley & Sons; 1993.

38. Holman JP: *Heat Transfer* (SI Metric Edition). New York: McGraw-Hill Book Company; 1989.

39. Jakob M: *Trans ASME* 1938, **60**:384-398.

40. Wierzbicki T, Abramowicz W: **Alexander revisited – a two folding elemnets modle of progressive crushing of tubes.** *Int J Solids Structures* 1983, **29**:3269-3288.

41. Andrews KRG, England GL, Ghani E: *Int J Mech Sci* 1983, **25**:687-696.

Patents

P1. Akiyama S, Imagawa K, Kitahara A, Nagata S, Morimoto K, Nishikawa T, Itoh M: **Foamed metal and method for producing same.** *US Patent No. 4 712 277;* 1987.

P2. Baumeister J, Schrader J: **Methods for manufacturing foamable metal bodies.** *German Patent DE 4 101 630;* 1991.

P3. Jin I, Kenny L, Sang H: **Method of producing lightweight foamed metal.** *US Patent No. 4 973 358;* 1990.